Prospect de-risking using CSEM

Joanne Suffert, EMGS, Volker Ullrich, EMGS, Marit Tørudbakken Jendal, RWE DEA Norge*

Summary

Controlled source electromagnetic (CSEM) data have been acquired along three 2D lines that cover two prospects offshore Norway. The purpose of the survey was to assess the hydrocarbon potential of these prospects as part of the exploration risking workflow

A cross-disciplinary interpretation of the CSEM data, including seismic interpretation, 3D inversion and post-survey 3D modeling, gave rise to a final geo-resistivity model that explains the data in a satisfactory way. Based on this interpretation, it was concluded that the prospects are likely to have either low hydrocarbon saturation or be water filled, and they were downgraded accordingly. A deep sill intrusion (2 km burial depth), crossed by one of the acquisition lines and expected to be highly resistive, was used as a calibration target. The sill intrusion was clearly detected and imaged by the 3D inversion, thus increasing our confidence in the data analysis.

Introduction

Controlled source electromagnetics (CSEM) is a remote sensing technique, which provides information about subsurface resistivity variations using electromagnetic energy. The method was demonstrated both theoretically (Kong *et al.*, 2002) and in practice by several calibration and commercial surveys (Ellingsrud *et al.*, 2002).

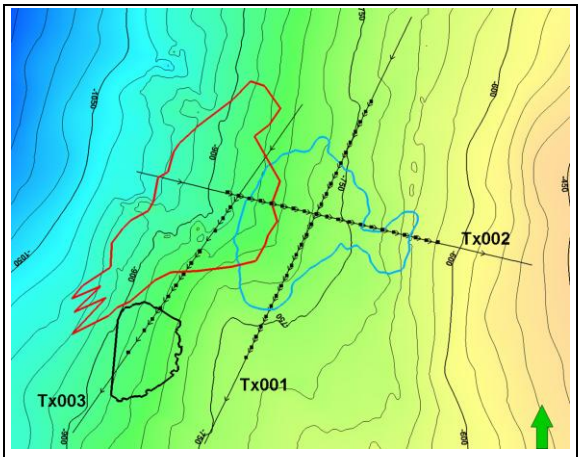

Figure 1: Survey layout. Black squares represent receiver positions. Prospect outlines are shown in red for prospect 1 (1 km burial depth) and blue for prospect 2 (2 km burial depth). The black outline marks the sill intrusion.

The concept of CSEM is based on the fact that the attenuation and velocity of electromagnetic energy is determined by formation resistivity and the source frequency. Hydrocarbon saturated sediments generally have higher resistivities than brine saturated sediments due to the fluid properties. However, subsurface resistivity anomalies are not restricted to hydrocarbon saturated sediments. Lithologies such as tight (cemented) sediments, limestone, salt and magmatic intrusions are known to have potentially high resistivities.

Survey layout and electromagnetic attribute analysis

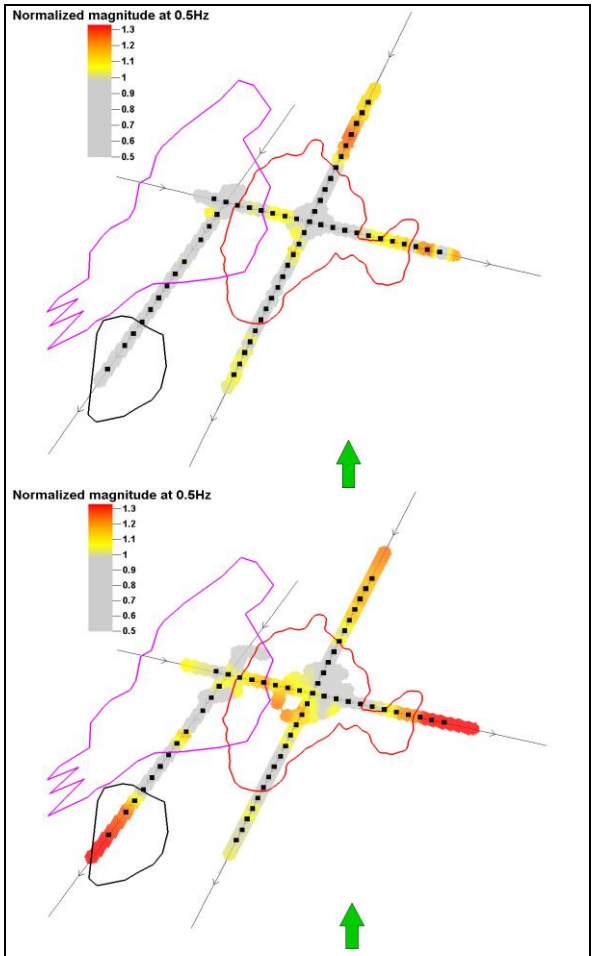

Figure 2: Normalized magnitude map at 3000m offset (top) and 6000m offset (bottom) at 0.5Hz. Prospect outlines are shown in pink for prospect 1 and red for prospect 2. The black outline marks the sill intrusion.

A total of 58 receivers were deployed along three receiver lines (Figure 1). The water depth in the area ranges from 500 m to 1100 m.
The source pulse was designed to focus the energy on three frequencies, 0.25Hz, 0.5Hz and 1.0Hz (Mittet *et al.*, 2007), in order to be able to image both shallow and deep targets, using high and low frequencies, respectively.
The dense receiver spacing (1.25 km along Tx001 and Tx002 and 1.5 km along Tx003) is very suitable for advanced processing such as 3D inversion to be performed. Azimuth data has been acquired at the line crossings, increasing the data coverage (Maaø *et al.*, 2007, Thrane *et al.*, 2007).

After standard processing, all data have been compared to a single reference receiver located in the southern part of line Tx001. This process is called normalization and provides a means of comparing responses recorded at different receiver locations. By calculating the normalized response for each receiver at a given source-receiver offset, resistive and conductive anomalies are identified along the survey line. The normalized values can be plotted in map view to locate the anomaly spatially. Such maps are shown in Figure 2, with relatively short offsets (3000 m) representing shallow regions of the subsurface and relatively long offsets (6000 m) describing deeper regions of the subsurface.

Several resistive anomalies are visible. Most of these anomalies appear at relatively short offsets, indicating shallow resistivity variation. Towards the southern part of line Tx003, one anomaly appears at longer offsets. A comparison between a receiver located on top of this anomaly and one outside is presented in Figure 3. The phase of the receiver located above this anomaly starts to decrease from 5 km offset, indicating a highly resistive layer at depth. Combined with the seismic interpretation, this anomaly corresponds spatially with the outline of a sill intrusion (black outline in Figure 2).

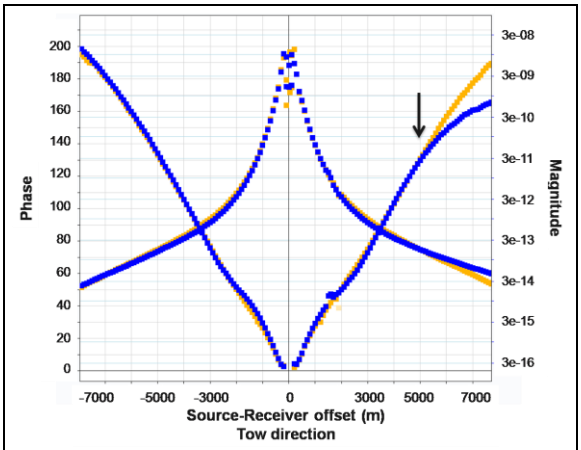

Figure 3: Magnitude and phase versus offset, comparing the reference receiver (orange) to a receiver located above the sill intrusion (blue).

3D inversion and 3D modeling results

3D modeling and 3D inversion were used to assess the resistivity distribution in the subsurface and to find the most probable resistivity values for the prospects.

Pre-survey sensitivity modeling, based on horizons from seismic interpretations and resistivity values from nearby wells, was performed to assess the response of potential reservoirs. In post-survey modeling, the main aim is to create the best possible background model and compare it's response with the real data. Commonly, the model

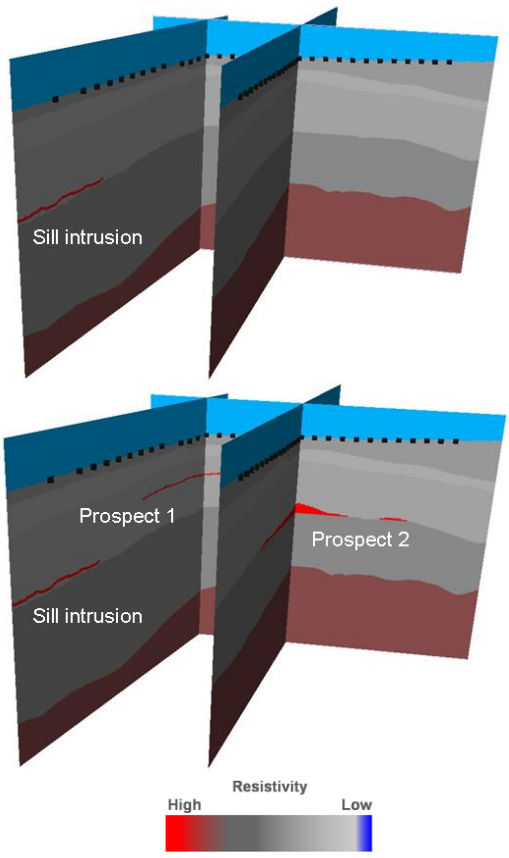

Figure 4: 3D background model (top) and 3D reservoir model (bottom). Color scale shows the vertical resistivities.

geometry remains similar to the pre-survey study but the background resistivities are replaced by values derived from 1D inversion (Roth *et al.*, 2007) or 1D modeling of several real receivers. The modeled resistivities show a clear indication of anisotropy (factor 2 to 4) in the shallow layers of the subsurface.
Direct comparison of real and modeled data are shown in Figure 6. The mismatch is calculated with the following formula, where *E* represents the electric field:

$$\varepsilon = \frac{\left| E_{measured} - E_{synthetic} \right|^2}{\left| E_{measured} \right|^2}$$

By introduction or removal of resistors, each prospect or any combination of them can be modeled and compared to the measured data (Figure 4 and Figure 6). We found that several of the measured resistive anomalies can be explained by our background model.

In parallel with 3D post-survey modeling, 3D inversion was performed along the three lines. The inversion of CSEM data aims at finding a resistivity model of the sub-surface that reproduces a set of observed data to within survey measurement accuracy.

Given the limited data coverage and measurement uncertainty of the survey, there are several resistivity models that explain the observed data. To obtain a more reliable resistivity model from this dataset, inversion was conducted using different start models and with varying frequency content. The results from these different inversions were then subjected to a number of consistency tests, and were then interpreted using any additional knowledge of the geology of the survey area.

The results shown here were obtained by inverting the three main frequencies (0.25Hz, 0.5Hz and 1.0Hz) and with a half-space start model of constant resistivity.

The data from the inversion results (Figure 5), show consistent results with the pre/post-survey 3D modeling. From the cross-sections, there is a relatively high resistivity in the upper part of the subsurface, followed by a lower resistivity interval. The resistivity then increases with depth. The upper part of the subsurface is expected to be anisotropic. Since the inline source-receiver configuration is primarily sensitive to vertical resistivity, we expect the resistivity distribution obtained by the 3D inversion to be more representative of the vertical resistivity distribution.

On line Tx003 a highly resistive anomaly is visible, starting approximately 2 km below mud-line. This anomaly accurately matches the depth of the interpreted sill intrusion.

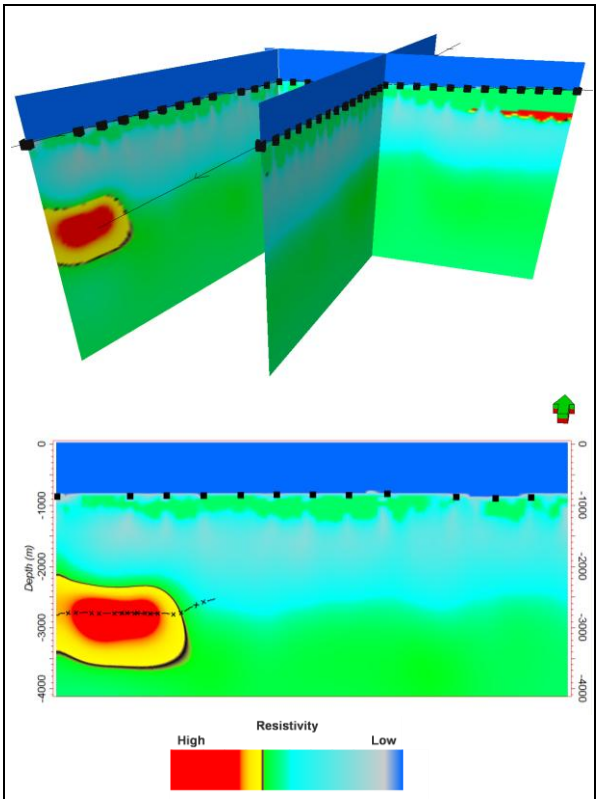

Figure 5: 3D inversion results along the three lines (top) and cross-section along line Tx003 (bottom). Black squares represent receiver positions. Red indicates areas of high resistivity while blue indicates areas of lower resistivity.

From the 3D inversion results, no anomalies related to the prospects are observed. Therefore a sensitivity study is essential in order to understand why we do not observe any resistive anomalies and which resistivities the prospects are likely to have.

Interpretation and integration

The resistive anomaly on line Tx002 (Figure 2), covering the eastern edge of prospect 2 and extending to the end of the towline, shows an increasing normalized magnitude response. Seismic horizons indicate an eastward thickening of the uppermost sediment layer (Figure 6, top). From 1D modeling and inversion we know that this layer is most probably anisotropic. When running an anisotropic 3D model with a horizontal resistivity of 2 Ωm and vertical resistivity of 4 Ωm in the top layer, the response from the pure background model is very similar to the measured data (Figure 6). Since the EM method is mainly sensitive to the vertical resistivity component and that the vertical resistivity is relatively high, the increase in thickness of the top layer explains the measured anomaly without

introducing any additional resistors. All other shallow anomalies within the survey area can be linked to this phenomenon.

Initially, 30 Ωm was the anticipated resistivity value in the two prospects. However, post-survey modeling showed that this was too high and only values below 10 Ωm fit the measured data (Figure 6). Prospects with 30 Ωm show a large misfit (blue areas) while the 10 Ωm case is not distinguishable from the pure background model.

This indicates that the prospects are either hydrocarbons with low saturation values or water filled sediments.

Discussion

Advanced imaging and 3D modeling were used in the post-survey workflow, leading to a satisfactory interpretation of the dataset.

The volcanic intrusion was detected in a spatially accurate position and served as a calibration for the area. All shallow anomalies could be explained by a pure background model only including anisotropy and thickness changes in the uppermost layer of the sedimentary column.

Even though this survey resulted in down-grading the prospects, it was rated as a success by the client since it freed resources for other projects and saved further exploration costs in the area.

Acknowledgements

We would like to thank RWE-DEA Norge for granting permission to publish the results of this survey. We would also like to thank all geophysicists and geologists at RWE-DEA Norge and EMGS that have contributed with their expertise and knowledge to the successful processing and interpretation of the data.

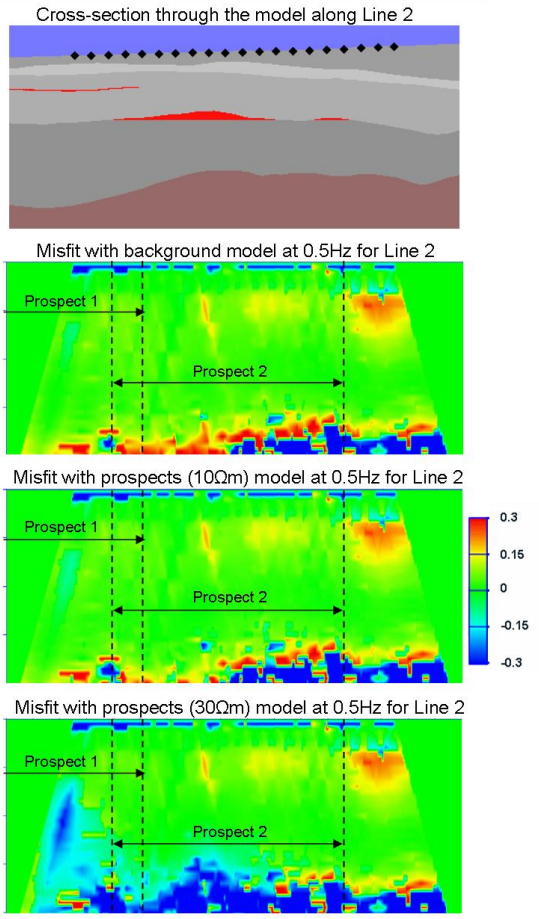

Figure 6: Cross-section along line 2 of the 3D resistivity model (top). Misfit plots between real and modeled data with background model - waterfilled sediment (top), with 10 Ωm prospects (middle) and 30 Ωm prospects (bottom).